

Vibrational modes, optical excitations, and phase transition of solid C₆₀ at high pressures

D. W. Snoke, Y. S. Raptis,* and K. Syassen

Max-Planck-Institut für Festkörperforschung, Heisenbergstrasse 1, 7000 Stuttgart 80, Germany

(Received 16 March 1992)

We have investigated the effect of pressure on the vibrational modes and optical response of C₆₀ and C₇₀ fullerene powder from several sources, via Raman spectroscopy and optical reflectivity measurements. Fullerene Raman peaks remain observable up to about 22 GPa, indicating that the fullerenes have stability comparable to that of hexagonal graphite under pressure. The Raman signal of this new phase after pressure release is that of amorphous carbon. We compare the reflectivity spectrum of this phase to that of the high-pressure phase obtained from graphite and conclude that the two high-pressure phases are different.

Interest in the chemical and physical properties of C₆₀ and C₇₀ fullerenes has continued to grow, following their synthesis in macroscopic amounts¹ and the reports of superconductivity of doped fullerenes with transition temperatures above 30 K.² At ambient conditions C₆₀ crystallizes in a face-centered-cubic (fcc) structure with a lattice constant of 14.17 Å.³ At 249 K solid C₆₀ undergoes a transition to simple-cubic (sc) structure involving orientational order of the C₆₀ molecules in the low-temperature sc phase.³ Pressure increases the order-disorder transition temperature, so that at room temperature C₆₀ has the sc phase at pressures above about 0.45 GPa.⁴ The pressure dependence of the lattice parameter of solid C₆₀ has been measured by x-ray diffraction;⁵ in that study it was shown that the C₆₀ balls remain stable up to about 20 GPa. The superconducting transition temperature of alkali-doped C₆₀ decreases under pressure,⁶ and the scaling of T_c with the lattice parameter is similar to that obtained by doping with different alkali metals.⁷

In this work we address two aspects of the high-pressure behavior of undoped fullerenes. The first concerns the change of electronic π - π^* transitions and intramolecular vibrational excitations induced by increasing intermolecular coupling. It is important to understand these properties of the undoped material because it is electron-phonon coupling which seems to be responsible for superconducting properties (see, e.g., Refs. 8–12). The second aspect of this work is the question of stability of the buckyballs with respect to denser modifications of carbon. For instance, sp^2 -bonded hexagonal graphite at $T=300$ K is known to have an ultimate stability range of 15–18 GPa, where it transforms to a disordered phase possibly with predominant sp^3 bonding (see Refs. 13 and 14 and earlier work cited therein). The carbon molar volume of C₆₀ fullerenes is about 35% larger than that of graphite. Therefore, in the case of fullerenes the application of pressure is an even stronger driving force for inducing phase changes.

Early x-ray studies showed that C₆₀ undergoes a structural phase transition to a phase of lower symmetry at about 20 GPa.⁵ No conclusion about the reversibility of the high-pressure phase could be made at that time. In a previous publication,¹⁵ we reported that a C₆₀-C₇₀ mixture transformed irreversibly to amorphous carbon above 20 GPa, based on Raman-scattering data. Following that report, electrical measurements¹⁶ confirmed the existence

of the high-pressure structural phase transition at around 20 GPa, and indicated an energy gap *increasing* with pressure. We report here that purified C₆₀ shows the same transition to amorphous carbon as previously reported for the C₆₀-C₇₀ mixture, and we find that this irreversible transition also appears in the reflectivity data. The reflectivity measurements provide an unambiguous identification of two of the optical gaps and their shifts with pressure.

We have looked at a mixture of C₆₀-C₇₀ (sample 1) and purified C₆₀ (samples 2, 3, and 4) obtained from several sources.¹⁷ The Raman results for C₆₀ were essentially the same for all the samples. Our data for C₇₀ were deduced from the data of the C₆₀-C₇₀ powder mixture (sample 1), knowing the C₆₀ results. Samples were either loaded into a gasketed diamond anvil cell without using any pressure medium or with chemically inert CsCl as a pressure medium, with similar results in each case. The pressure was calibrated¹⁸ by the luminescence of ruby powder or chips distributed over the sample volume. From the ruby luminescence, the variation of pressure over the sample volume was at most 1 GPa.

Raman scattering. For the Raman measurements we have used the 530.9-nm Kr⁺ laser line or the 514.5-nm Ar⁺ laser line and a Spex Triplemate spectrometer in combination with a position-sensitive photomultiplier, calibrated using neon emission lines to give an absolute wave number within 2 cm⁻¹ over the entire range of interest. The optimum laser power was found to be less than 5 mW, measured in front of the pressure cell. Due to the unavoidable backward scattering through the diamond of the high-pressure cell, the frequency range from 1250 to 1400 cm⁻¹ was covered by the very strong 1332 cm⁻¹ diamond peak, obscuring one C₆₀ and four C₇₀ peaks expected in this range.

We have measured the Raman spectra both for pressure increasing and decreasing for several maximum pressures ranging from 5 to 42 GPa. In Fig. 1(a) we show characteristic high-frequency (1400–1700 cm⁻¹) Raman spectra of C₆₀ (source 3) at four different pressures (0.7, 5.3, 10.1, and 15.6 GPa) as pressure is increased, and again at atmospheric pressure after the pressure has been released from a maximum of 21 GPa. For maximum pressures less than 22 GPa the zero-pressure spectrum is recovered after pressure release, except for spectral

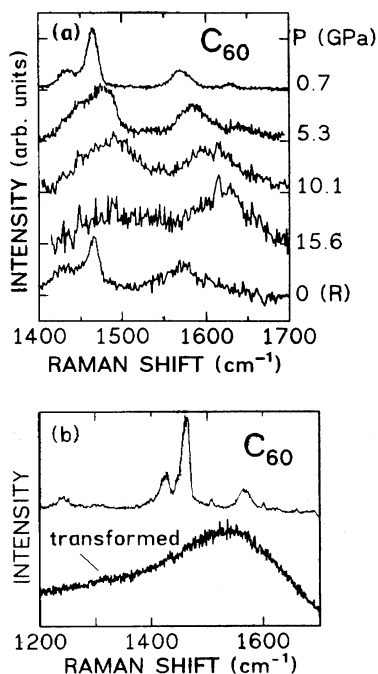


FIG. 1. (a) The high-frequency Raman spectra of C_{60} (sample 3) at room temperature at several pressures in a diamond anvil cell. The last curve, labeled (R), is the Raman spectrum of the same sample after removal from the diamond anvil cell after reaching a maximum pressure of 21 GPa. (b) The high-frequency Raman spectra of C_{60} (sample 4) at atmospheric pressure and of the transformed phase after pressure release from 42 GPa. The average signal for this spectrum is one count per ten seconds per channel at 1 mW laser power.

broadening, as seen in Fig. 1(a), and a decrease in intensity, discussed below. We conclude that at least some fraction of the C_{60} keeps its identity up to pressures of 22 GPa. This is remarkable, since sp^2 -bonded graphite under similar experimental conditions is known to have an ultimate stability limit of 15–18 GPa.^{13,14}

For pressures greater than about 13 GPa but less than 22 GPa, an irreversible decrease in Raman intensity of all lines is observed. Raman intensity on return to atmospheric pressure decreases continuously as maximum pressure increases, until no fullerene signal returns when pressures have exceeded 22 GPa. We infer that starting at pressures of around 13 GPa some fraction of the fullerenes undergoes an irreversible transition, with increasing fraction as pressure is increased. In x-ray studies,⁵ transition to the high-pressure phase at less than 20 GPa was correlated with the existence of uniaxial stresses, and this may be the case here since the applied pressure is not purely hydrostatic in our experiments.

For pressures higher than 22 GPa, the highest-frequency two-peak feature of our samples merges into a single broad band around 1600 cm^{-1} , which is then observed up to 42 GPa, the highest pressure achieved in our measurements. After release of the pressure down to 1 atm, and removal from the diamond anvil cell, the Raman spectrum can be clearly identified as that of amorphous carbon,^{19–21} with a maximum at 1550 cm^{-1} . The spec-

trum of sample 4 after pressure release from 42 GPa and removal from the diamond anvil cell is shown in Fig. 1(b). This spectrum is durable after exposure to air, and it is the same for all laser powers up to 10 mW. None of the fullerene peaks at zero pressure are recovered. The shift of the high-frequency maximum from 1700 cm^{-1} at around 40 GPa down to 1550 cm^{-1} at atmospheric pressure agrees with previous Raman data from amorphous carbon at high pressure.²² When some fraction of solvent used to separate the fullerenes remains in the samples (samples 1 and 2), a second peak at 1380 cm^{-1} appears, and the high-frequency peak narrows and shifts to higher energy.¹⁵ This altered spectrum is associated with the presence of hydrogen in amorphous carbon,^{20,21} also produced by laser irradiation of carbon in air.¹⁹ Although only the spectrum of amorphous carbon is seen, the possibility still exists that the observed spectrum corresponds to only some fraction of the transformed material. We emphasize, however, that Raman scattering from the transformed material provides no evidence for the presence of cubic or hexagonal diamond.

In Fig. 2 we show the pressure dependence of selected modes of C_{60} and C_{70} in the pressure range below the complete phase transition to amorphous carbon. We list the average pressure coefficients of these modes, as well as others, in Table I. The error in the pressure coefficients is on average $0.5\text{ cm}^{-1}/\text{GPa}$.

The ir- and Raman-active internal modes have been calculated^{23–25} and measured^{9,26} at ambient conditions. For C_{60} the I_h (icosahedral) symmetry implies ten Raman-active (two nondegenerate A_g and eight fivefold-degenerate H_g) modes.^{23,24} Apart from those obscured by the diamond line, we see the same C_{60} Raman frequencies for these Raman-allowed modes at atmospheric pressure as reported for C_{60} film on suprasil slides,²⁶ within a few wave numbers. In addition to the allowed Raman modes, we also see forbidden, infrared-active T_{1u} modes at 525 and 575 cm^{-1} . All of the Raman lines persist up to a pressure of 6 GPa. Above that pressure, the 421, 491, and 1431 cm^{-1} allowed lines and the forbidden lines become too weak, or broad, to observe. In Table I we list for comparison the zero-pressure mode frequencies and assign-

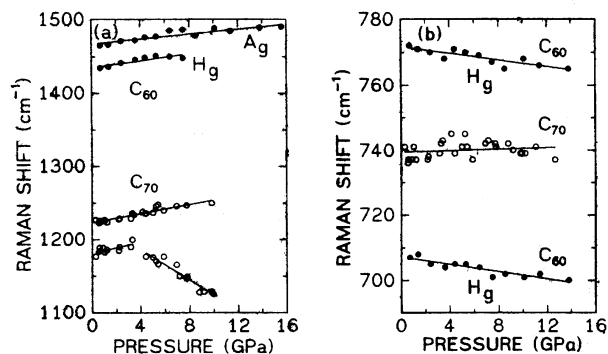


FIG. 2. Pressure dependence (a) of high-frequency Raman modes and (b) of medium-frequency modes of C_{60} and C_{70} . The solid lines correspond to least-squares fits of a linear pressure dependence. The 1182-cm^{-1} mode is fit in two segments because of the sign change of the slope.

TABLE I. Pressure dependence of selected Raman lines of C_{60} (top part) and C_{70} (lower part). Pressure coefficients correspond to average values for the pressure ranges where the modes could be observed.

	ω_i (cm^{-1})	$\partial\omega_i/\partial P$ ($\text{cm}^{-1}/\text{GPa}$)	Ref. 26	Assignment
C_{60}	268	1.1	273	$H_g(1)$
	421	2.4	437	$H_g(2)$
	491	0.94	496	$A_g(1)$
	525	-0.45	527	T_{1u}
	707	-0.55	710	$H_g(3)$
	772	-0.50	774	$H_g(4)$
	1431	2.4	1428	$H_g(7)$
	1465	1.7	1470	$A_g(2)$
1570	3.7	1575	$H_g(8)$	
C_{70}	256	1.65	261	
	517	0.38	501	
	564	-0.06	573	
	740	0.12	739	
	1065	1.1	1062	
	1182	4, -10.3	1186	
	1224	3.2	1231	
	1370	1.1	1370	
	1513	4.5	1517	
	1567	2.73	1569	

ments from Ref. 26. Our zero-pressure frequencies agree slightly better with those reported recently in Ref. 9.

Of the low-frequency modes of C_{60} , the $H_g(2)$ mode at 421 cm^{-1} shows the largest shift with pressure. Most notable is the behavior the two intermediate-frequency $H_g(3)$ and $H_g(4)$ modes of C_{60} and the forbidden T_{1u} mode, which soften with increasing pressure. In the high-frequency range all the observed modes show a positive frequency shift with increasing pressure; the largest overall shift is observed for the $H_g(8)$ mode at 1570 cm^{-1} .

A total of 53 Raman-active modes have been calculated²⁵ for the less symmetric C_{70} , assuming a D_{5h} symmetry. In Table I we list only those modes which can clearly be identified as belonging to C_{70} in the mixture of sample 1, due to substantial spectral separation from the C_{60} lines or much greater intensity, as measured in Ref. 26.

The 1186-cm^{-1} mode of C_{70} has a peculiar change of sign of the slope at 4 GPa. In the corresponding frequency range of the C_{60} spectrum there are two H_g lines (1099 and 1250 cm^{-1}),²⁶ which are the threshold for passing from the low-frequency bond bending (radial atomic motion) to the high-frequency bond stretching (tangential atomic motion). Possibly for the less symmetric C_{70} molecule the 1186-cm^{-1} mode changes its vibrational character at around 4 GPa.

Reflectivity measurements. We have measured the absolute reflectivity spectrum in the visible region with the sample in direct optical contact with the diamond window, using a spectrometer configuration similar to that of Ref. 27. In Fig. 3(a) we show reflectivity spectra for C_{60} (sample 3) at various pressures up to 31 GPa. The lowest-pressure spectrum is consistent (after correction for the

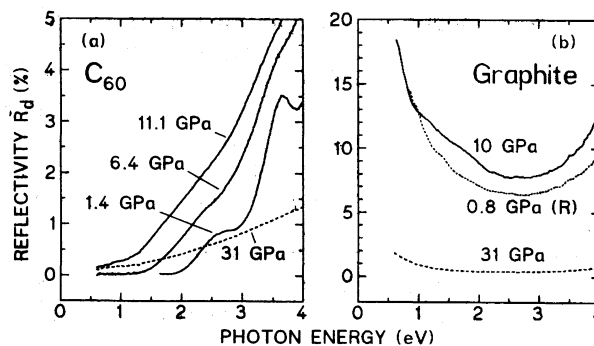


FIG. 3. (a) The absolute reflectivity of C_{60} (sample 3) at 1.4, 6.4, 11.1, and 31 GPa as pressure is increased. (b) The absolute reflectivity of graphite at 10 and 31 GPa as pressure is increased, and at 0.8 GPa following pressure release from 31 GPa. The sample reverts to a graphitelike phase, unlike the fullerenes.

different refractive index matching at the sample surface) with that calculated from ellipsometry data for free-standing samples of purified C_{60} .²⁸ Within the accessible spectral range we observe two reflectivity bands corresponding to optical transitions at about 2.5 and 3.5 eV. Since the intermolecular interactions are weak, these transitions can be assigned on the basis of a molecular orbital scheme.²⁹ The highest occupied molecular-orbital-lowest unoccupied molecular-orbital gap of C_{60} corresponds to a symmetry forbidden $h_u \rightarrow t_{1u}$ transition. Thus, the lowest-energy reflectivity band at 2.5 eV should be assigned to the next higher transition, which is the $(h_u + g_u) \rightarrow t_{1g}$ transition.^{28,30,31} Since the 3.5-eV transition becomes weaker with increasing alkali-metal doping,^{31,32} the final state of this transition appears to be the lowest unoccupied t_{1u} state. This suggests that the 3.5-eV transition corresponds to $(h_g + g_g) \rightarrow t_{1u}$ excitations.

With increasing pressure we observe a pronounced broadening of the two optical transitions and an overall redshift of the broadened reflectivity edge. This redshift is reversible for maximum pressures below 11 GPa, although for maximum pressures above 6 GPa the structure in the reflectivity spectrum seen at low pressures becomes irreversibly washed out to some degree. We attribute the broadening of the reflectivity edge with increasing pressure mainly to the increasing width of molecular states. At ambient pressure the bandwidth of the relevant states is calculated to be about 0.5 eV.^{33,34} A broadening by at least a factor of 2 in 10 GPa is to be expected, since in the case of graphite the interlayer overlap interaction shows a similar increase with pressure.¹⁴

Up to about 10 GPa, the onset of allowed interband absorption remains well resolved in the reflectivity spectra. The average redshift of the low-energy tail in the reflectivity amounts to about -1 eV in 10 GPa. For the reported bulk modulus of C_{60} of 18 GPa (Ref. 5) this implies an average deformation potential of 1.8 eV. This pressure shift is large compared with that of $\pi\text{-}\pi^*$ transitions in aromatic hydrocarbons, but less than the initial absorption edge shift in polyacetylene under pressure.³⁵ If the assignment of optical transitions given above is correct, this result implies a high sensitivity of the $(h_u + g_u) \rightarrow t_{1g}$ transition to intermolecular coupling.

The pressure-induced band broadening is expected to account for a certain fraction of the red shift. However, there may be a second effect contributing to the strong redshift of the low-energy excitations, which is of intramolecular nature and involves changes in internal coordinates. For instance, a decrease of bond alternation is expected to result in a lowering of the relevant optical excitation energies.^{34,36}

Above 13 GPa an overall, irreversible decrease in reflectivity occurs as pressure increases. The irreversible nature of the high-pressure phase transition, seen in the Raman data, is also seen in these data, since the structure of the spectrum at atmospheric pressure does not return after unloading from 31 GPa and the overall reflectivity remains low.

In Fig. 3(b) we compare the spectrum of the transformed material to that of the high-pressure phase of graphite, which has also been postulated to be amorphous.³⁷ Clearly, the two phases are not the same. Although at 31 GPa the transformed graphite spectrum has a low absolute reflectivity comparable to that of the new phase of the fullerenes, when the pressure is released the graphite phase returns.

Conclusions. We have seen that fullerenes are remarkably stable at room temperature—we have been able to measure a reliable pressure dependence of several Raman lines up to pressures of 20 GPa. At around 22 GPa the two strongest high-frequency peaks merge into one broad-

band, which persists up to 42 GPa, indicating no further phase transition. This change in the Raman spectrum is not reversible upon releasing pressure. A comparison with Raman spectra of various carbon forms shows that the new phase produced from fullerenes consists mainly of amorphous carbon. The presence of solvent mixed with the fullerenes can be detected in the Raman spectrum of the amorphous phase.

Further evidence for an irreversible phase transition comes from measurements of the absolute reflectivity spectrum. Below 11 GPa we observe a reversible redshift of 0.1 eV/GPa of the lowest optical gap, which we assign to the $(h_u + g_u) \rightarrow t_{1g}$ transition. Above 13 GPa a continuous, irreversible decrease in absolute reflectivity occurs. Comparison of the reflectivity spectra of the transformed fullerenes and that obtained from graphite at high pressures shows that the new, irreversible phase is not the same as the reversible high-pressure phase of graphite.

We thank G. Stollhoff for fruitful discussions. We also thank P. Bernier, A. Zahab, S. Roth, W. Hönle, H. Schmidt, A. Mittelbach, J. Fink, and E. Sohmen for fullerene samples and for useful interactions. One of us (D.W.S.) thanks the Alexander von Humboldt Foundation for financial support and the Max-Planck-Institut for its hospitality. Y.S.R. is also indebted to the Max-Planck-Institut for its hospitality.

*On leave from Physics Department, National Technical University, 15773 Zografou, Greece.

¹W. Krätschmer, K. Fostiropoulos, and D. R. Huffman, *Chem. Phys. Lett.* **170**, 167 (1990).

²K. Tanigaki *et al.*, *Nature (London)* **352**, 222 (1991).

³P. A. Heiney *et al.*, *Phys. Rev. Lett.* **66**, 2911 (1991).

⁴G. A. Samara *et al.*, *Phys. Rev. Lett.* **67**, 3136 (1991).

⁵S. J. Duclos *et al.*, *Nature (London)* **351**, 380 (1991).

⁶G. Sparr *et al.*, *Science* **252**, 1829 (1991).

⁷R. M. Fleming *et al.*, *Nature (London)* **352**, 787 (1991).

⁸T. W. Ebbesen *et al.*, *Nature (London)* **355**, 620 (1992).

⁹M. G. Mitch, S. J. Chase, and J. S. Lannin, *Phys. Rev. Lett.* **68**, 883 (1992).

¹⁰M. Schluter *et al.*, *Phys. Rev. Lett.* **68**, 526 (1992).

¹¹C. M. Varma, J. Zaanen, and K. Raghavachari, *Science* **254**, 989 (1991).

¹²I. I. Mazin *et al.*, *Phys. Rev. B* **45**, 5114 (1992).

¹³M. Hanfland, H. Beister, and K. Syassen, *Phys. Rev. B* **39**, 12598 (1989).

¹⁴M. Hanfland, K. Syassen, and R. Sonnenschein, *Phys. Rev. B* **40**, 1951 (1989).

¹⁵Y. S. Raptis *et al.*, in *Proceedings of the European High Pressure Research Group Conference, Thessaloniki, Greece, 1991* [High Pressure Res. (to be published)].

¹⁶M. Nunez Regueiro *et al.*, *Nature (London)* **354**, 289 (1991).

¹⁷A mixture of C₆₀-C₇₀ was obtained from P. Bernier and A. Zahab of the Université des Sciences et Technologies de Longuedoc (sample 1), while purified samples of C₆₀ were obtained from W. Hönle, H. Schmidt, and A. Mittelbach of the Max-Planck-Institut für Festkörperforschung, Stuttgart (sample 2), from E. Sohmen of the Kernforschungszentrum

Karlsruhe (INF) (sample 3), and from Strem Chemicals, Kehl, Germany (sample 4).

¹⁸H. K. Mao *et al.*, *J. Appl. Phys.* **49**, 3276 (1978).

¹⁹A. Richter *et al.*, *J. Non-Cryst. Solids* **88**, 131 (1986).

²⁰J. Wagner *et al.*, *Phys. Rev. B* **40**, 1817 (1989).

²¹M. Yoshikawa *et al.*, *Solid State Commun.* **66**, 1177 (1988); *Appl. Phys. Lett.* **52**, 1639 (1988).

²²A. F. Goncharov and V. D. Andreev, *Zh. Eksp. Teor. Fiz.* **100**, 251 (1991) [*Sov. Phys. JETP* **73**, 140 (1991)].

²³R. E. Stanton and M. D. Newton, *J. Phys. Chem.* **92**, 2141 (1988).

²⁴D. E. Weeks and W. G. Harter, *J. Chem. Phys.* **90**, 4744 (1989).

²⁵Z. Slanina *et al.*, *J. Mol. Struct.* **202**, 169 (1989).

²⁶D. S. Bethune *et al.*, *Chem. Phys. Lett.* **179**, 181 (1991).

²⁷K. Syassen and R. Sonnenschein, *Rev. Sci. Instrum.* **53**, 633 (1982).

²⁸M. K. Kelly *et al.* (unpublished).

²⁹S. Satpathy, *Chem. Phys. Lett.* **130**, 545 (1986).

³⁰M. Matus, H. Kuzmany, and W. Krätschmer, *Solid State Commun.* **80**, 839 (1991).

³¹T. Pichler *et al.*, *Solid State Commun.* (to be published).

³²E. Sohmen, J. Fink, and W. Krätschmer, *Europhys. Lett.* (unpublished).

³³S. Saito and A. Oshiyama, *Phys. Rev. Lett.* **66**, 2637 (1991).

³⁴S. Satpathy *et al.*, *Phys. Rev. B* (to be published).

³⁵A. Brillante *et al.*, *Physica B* **139/140**, 516 (1986).

³⁶H. Scherrer and G. Stollhoff (unpublished); G. Stollhoff (private communication).

³⁷A. F. Goncharov, *High Pressure Res.* (to be published).